Design and Behavior of Multi-Orientation Fillet Weld Connections

LOGAN J. CALLELE, ROBERT G. DRIVER and GILBERT Y. GRONDIN

Abstract

Several independent research projects have demonstrated that the strength and ductility of fillet welds are a function of the angle between the weld axis and the line of action of the applied load. It has been demonstrated that transverse welds are about 50% stronger than longitudinal welds, but have considerably lower ductility. This difference in behavior can have a significant impact on the design of welded connections with multiple weld orientations within the same joint. Tests on concentrically loaded welded double lapped joints have recently been conducted to investigate the strength of connections with multiple weld segments of different orientations. The tests indicate that these joints possess capacities significantly lower than the sum of the individual weld segment strengths. The tested connections' capacities are a function of the interaction of the load versus deformation characteristics of the individual weld segments. A general approach for the design of welded joints that combine welds in various directions that reflects the individual segments' load versus deformation interaction is recommended.

Keywords: multi-orientation fillet welds, transverse welds, longitudinal welds, connections, steel construction.

INTRODUCTION

Recent research conducted at the University of Alberta by Deng et al. (2006) and Ng et al. (2004) have verified the suitability of the current North American design equations for evaluating fillet weld strength: clause 13.13.2.2(b) of S16–01 (CSA, 2001) and equations J2-4 and J2-5 of the AISC *Specification* (AISC, 2005). That research examined concentrically loaded fillet-welded connections fabricated such that all the welds had the same loading orientation—these types of connections are referred to as single-orientation fillet weld (SOFW) connections in this paper. However, fillet-welded connections commonly include welds at different orientations to the applied load—these types of connections are referred to as multi-orientation fillet weld (MOFW) connections.

It is well-known that fillet welds oriented transverse to the applied load exhibit higher unit strengths but generally lower deformation capacity than longitudinal fillet welds (Butler, Pal and Kulak, 1972; Lesik and Kennedy, 1990). This paper examines how the strength and behavior of MOFW connections with equal weld sizes in the various weld segments are affected by the variation in strength and deformation capacity of fillet welds with respect to loading orientation. A method of designing concentrically loaded MOFW connections for any given critical segments (weld segments with an orientation closest to 90°) and noncritical weld segments (the remaining weld segments in the connection) is presented. This design procedure is compared with the results of 19 MOFW connection tests conducted as part of this research program.

Logan Callele, Structural Engineer, Waiward Steel Fabricators Ltd., 10030-34 St., Edmonton, AB, T6B 2V5, Canada (corresponding author). E-mail: logan.callele@waiward.com

Robert G. Driver, Professor, Department of Civil and Environmental Engineering, 3-133 Natural Resources Engineering Facility, University of Alberta, Edmonton, AB, T6G 2W2, Canada. E-mail: rdriver@ualberta.ca

Gilbert Y. Grondin, Professor, Department of Civil and Environmental Engineering, 3-025 Natural Resources Engineering Facility, University of Alberta, Edmonton, AB, T6G 2W2, Canada. E-mail: ggrondin@ualberta.ca

BACKGROUND

Previous research on eccentrically loaded fillet weld connections provides information on fillet weld deformation capacity and load–response behavior (e.g., Butler et al., 1972; Lesik and Kennedy, 1990). These two research programs investigated the behavior of eccentrically loaded connections using the method of the instantaneous center of rotation. This method of analysis requires a way of predicting the strength, deformation capacity, and load–deformation behavior of fillet welds of any loading orientation.

The fillet weld deformation capacity and load–deformation behavior used by Butler et al. (1972) and Lesik and Kennedy (1990) for transverse and longitudinal fillet welds are shown in Figure 1, where Δ is the deformation of the weld and d is the leg size. These curves reveal that if both longitudinal and transverse welds are used in a single connection such that all of the welds undergo the same deformation, the longitudinal welds would not reach their ultimate strength by the time the transverse welds have reached theirs. Thus, the lower deformation capacity of the transverse fillet welds limits the connection capacity.

The effect of fillet weld deformation capacity on connection capacity has also been examined by Manuel and Kulak (2000) for transverse and longitudinal welds. This work investigated the behavior of connections combining high-strength structural bolts and fillet welds. These researchers observed that in connections where both transverse and longitudinal welds are present, the longitudinal welds reach only 85% of their predicted ultimate strength at the ultimate capacity of the connection. They stated that the capacity of the longitudinal fillet welds at the connection capacity is directly related to fracture deformation of the transverse fillet welds.

The work of Butler et al. (1972), Lesik and Kennedy (1990), and Manuel and Kulak (2000) indicates that the deformation capacity and load–deformation characteristics of fillet welds affect the capacity of MOFW connections and that this behavioral aspect should be taken into account in design. One common connection that is composed of fillet welds with more than one loading orientation is one with both transverse and longitudinal welds. An examination of Figure 1 shows that the capacity of a connection composed of both transverse and longitudinal fillet welds would be affected primarily by the deformation capacity of the transverse fillet weld and, to a lesser degree, the load–deformation characteristics of the longitudinal fillet weld. The load–deformation response proposed by Butler et al. (1972) indicates that the longitudinal weld will contribute 94% of its capacity to the connection capacity, whereas that of Lesik and Kennedy (1990) indicates that the longitudinal weld will contribute 80% of its capacity. This discrepancy is primarily a result of the greater transverse fillet weld deformation capacity predicted by Butler et al. (1972). The larger deformation capacity of the transverse weld allows for more deformation to be available to develop the longitudinal fillet weld capacity.

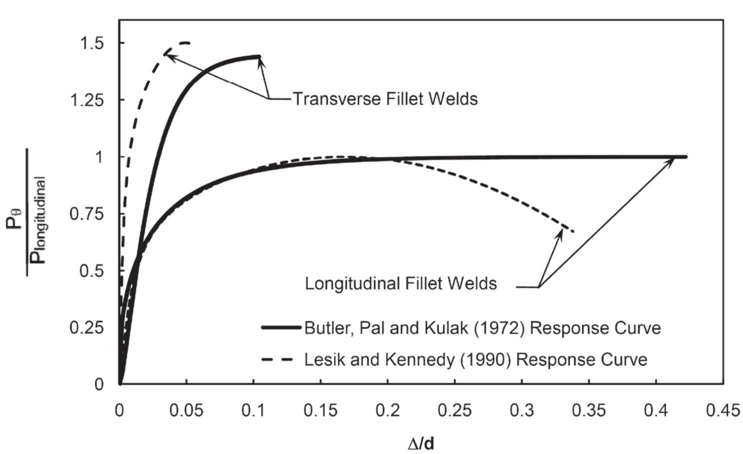

Fig. 1. Previous research into fillet weld behavior.

The significance of the effect of fillet weld deformation capacity and load–deformation response on the capacity of MOFW connections requires that an accurate estimate of these two fillet weld characteristics be obtained. The research programs by Butler et al. (1972), Lesik and Kennedy (1990), and Manuel and Kulak (2000) were all based upon fillet-welded connections fabricated using the shielded metal arc welding (SMAW) process. However, the flux cored arc welding (FCAW) process is much more prevalent in current structural steel fabrication practice. The SMAW process can produce fillet welds that have higher toughness than the FCAW process (Deng et al., 2006). This difference in toughness raises the question as to whether or not the fillet weld load–deformation responses developed for SMAW fillet welds are adequate to analyze connections fabricated with FCAW fillet welds at multiple loading orientations.

Two recent research projects at the University of Alberta investigated the accuracy of the current fillet weld strength predictions by North American design specifications (Ng et al., 2004; Deng et al., 2006). The primary focus was to investigate whether or not the strength of concentrically loaded SOFW connections fabricated using the FCAW process could be estimated adequately and safely by current North American design provisions. The fillet weld deformation capacity and load–deformation characteristics from the work of Deng et al. (2006) are used to analyze the tested connections from the current research on FCAW fillet weld connections with more than one fillet weld loading orientation.

EXPERIMENTAL INVESTIGATIONS

Two connection arrangements were tested to investigate welded connections containing more than one fillet weld loading orientation. The first connection type combined transverse and longitudinal fillet welds ("TL" specimens), while the second combined transverse and 45° fillet welds ("TF" specimens). Both connections types were fabricated by welding a lap plate on both sides of two main plates. The connection geometries and weld information are given in Table 1 and Figures 2 and 3.

Of the 19 MOFW connection specimens tested, 11 were TL specimens and 8 were TF specimens. The default nominal weld leg size is 12.7 mm (½ in.), and the suffix "a" is used to denote where 7.9 mm (5/16 in.) fillets were used instead. Four TF specimens and four TFa specimens were tested. The TL specimens are also distinguished in their designation by the longitudinal weld length: four TL50 specimens, four TL50a specimens and three TL100 specimens.

In order to analyze the MOFW connection specimens, it was necessary to conduct a complementary testing program

Table 1. Test Specimen Geometry and Weld Information					
Nominal Dimensions (See Figures 2 and 4)	**Specimen Designation**				
	TL50	**TL50a**	**TL100**	**L100**	**L150**
Length of test region, L_T (mm)	51	51	102	102	152
Length of reinforced region, L_R (mm)	102	102	152	203	254
Plate thickness, t (mm)	44	44	70	41	70
Main plate length, X (mm)	457	457	610	610	610
Fillet weld leg size (mm)	12.7	7.9	12.7	12.7	12.7
Number of passes	3	1	3	3	3

to supplement the information from Deng et al. (2006). The test specimens were double lap plate connections with only longitudinal fillet welds ("L" specimens) or transverse fillet welds ("T" specimens); Figures 4 and 5, along with Table 1, provide the geometric and welding information. Three L100, L150, and T specimens were fabricated for a total of nine extra specimens that make up the complementary tests. The complementary tests were chosen to be SOFW connections that were fabricated with identical weld filler metal, load orientation and nominal size as an individual segment from the MOFW connections. The observed behavior of the complementary tests thus formed the basis of the assumed behavior of the individual segments of the MOFW connections that were tested.

The nine complementary tests are of a similar arrangement to those presented in Deng et al. (2006) with the following exceptions: the L100 and L150 tests have longer longitudinal welds than the L1, L2 and L3 tests of Deng et al. (2006), and the transverse weld specimens' connection plates remained elastic, whereas those tested by Deng et al. (2006) yielded at, or prior to, reaching the connection capacity.

All 28 specimens (i.e., both the complementary and MOFW connection specimens) were fabricated with E70T-7 filler metal and with plates that were thick enough to ensure that plate yielding did not take place during testing. E70T-7 wire is a self-shielding wire used for FCAW. No start/stops were permitted within the tested welds during fabrication of all specimens. Test specimens TL50, TL50a,

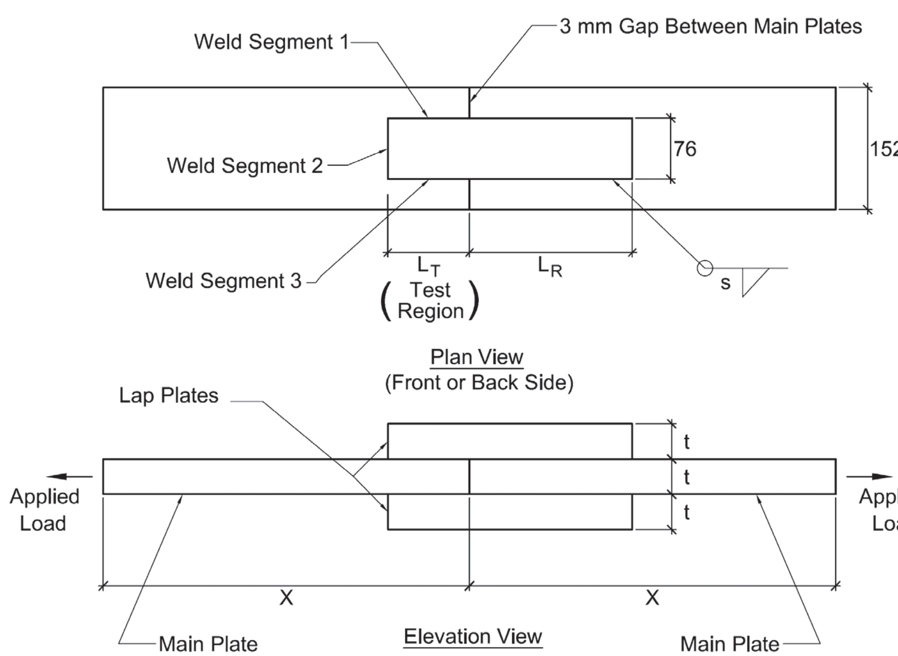

Fig. 2. Typical lap plate connection combining transverse and longitudinal welds (TL specimens).

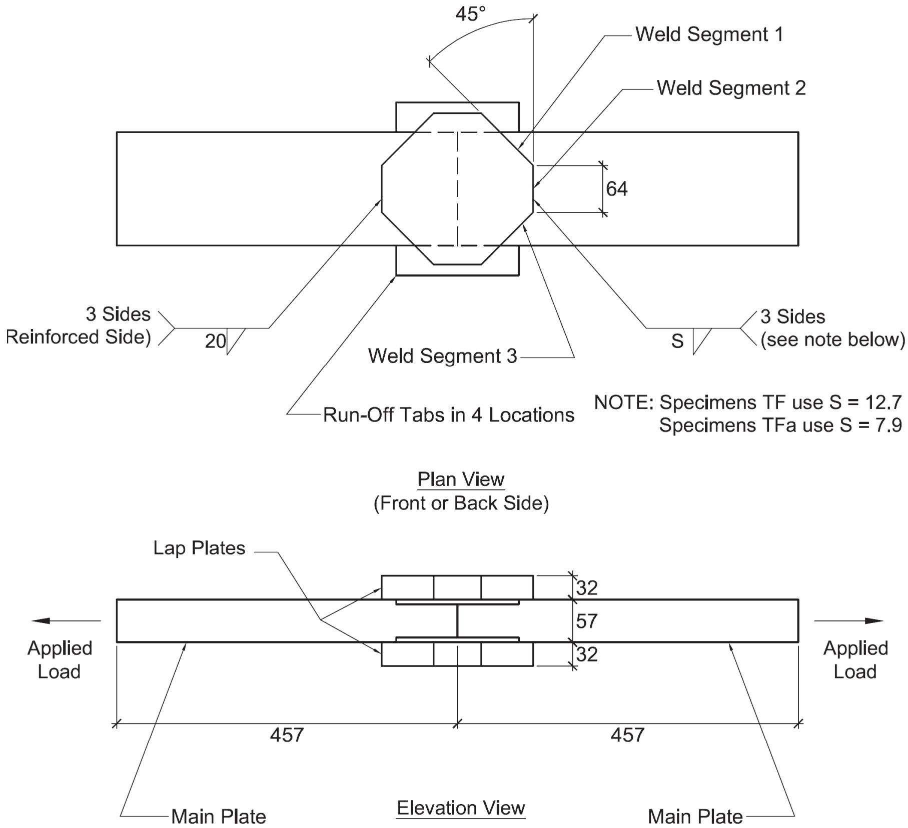

Fig. 3. TF and TFa specimens.

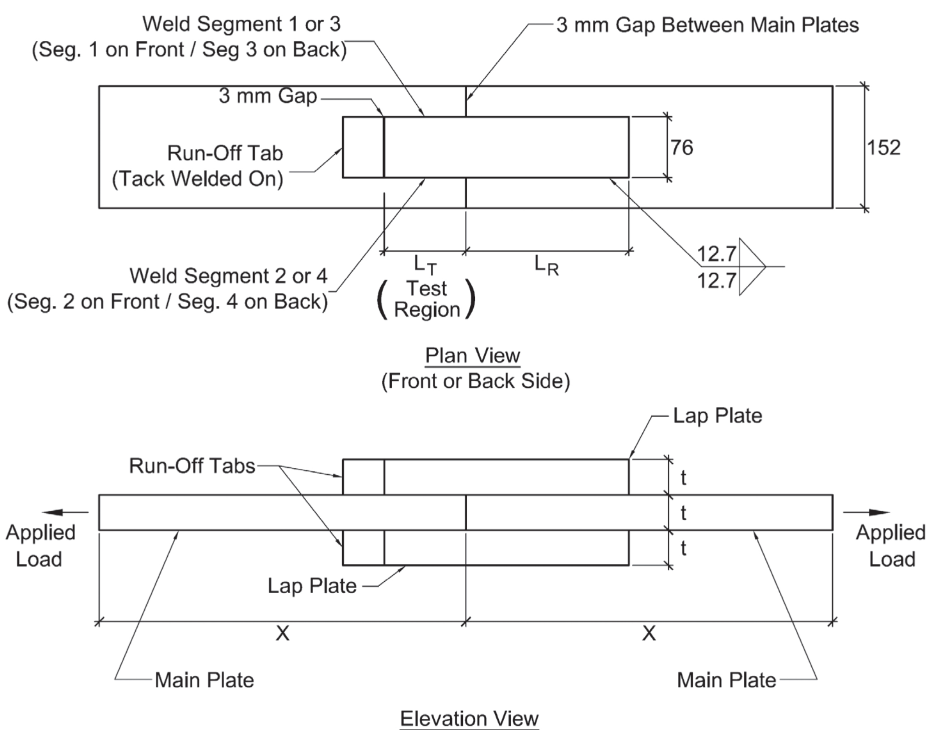

Fig. 4. Complementary test longitudinal fillet weld (L) specimen.

TF and TFa were fabricated from one heat of E70T-7 wire, while the remaining specimens were fabricated from a different heat. To establish the ultimate strength of the E70T-7 weld metal from both heats, six all-weld-metal tension coupons were fabricated and tested. These coupons had a 50-mm (2-in.) gage length and were fabricated in accordance with Clause 9 of ANSI/AWS A5.20/A5.20M:2005 (AWS, 2005). The plates used in the fabrication of all specimens met the requirements of ASTM A572 grade 50 and CAN/CSA-G40.21 350W steel.

Prior to testing, all test fillet welds were measured. Values for the measured fillet weld main plate leg (MPL) and lap plate leg (LPL) sizes, as well as the measured weld segment lengths, are given in Tables 2 through 5 for all of the specimens tested. Figure 6 provides a description of MPL and LPL and their relationship to the minimum throat dimension (MTD). The MTD neglects both the root penetration and the weld reinforcement, as is typically done in design. It should be noted, however, that fillet welds generally do not fail on the minimum throat plane (Miazga and Kennedy, 1989) and that the MTD values are used to normalize the test data as shown in the subsequent section. For further information on the fillet weld measurements, including post-fracture measurements, refer to Callele et al. (2005).

The testing of each specimen took place by loading the connection in concentric tension until rupture of one or all of the fillet welds occurred. The tests were carried out quasi-statically in a universal testing machine under displacement control. At several points during testing the displacement was held constant until the load stabilized. Linear variable differential transformers (LVDTs) were used to measure the fillet weld deformations in the direction of the applied load. Typical specimen test setup is shown in Figure 7. For further information on the test setup refer to Callele et al. (2005).

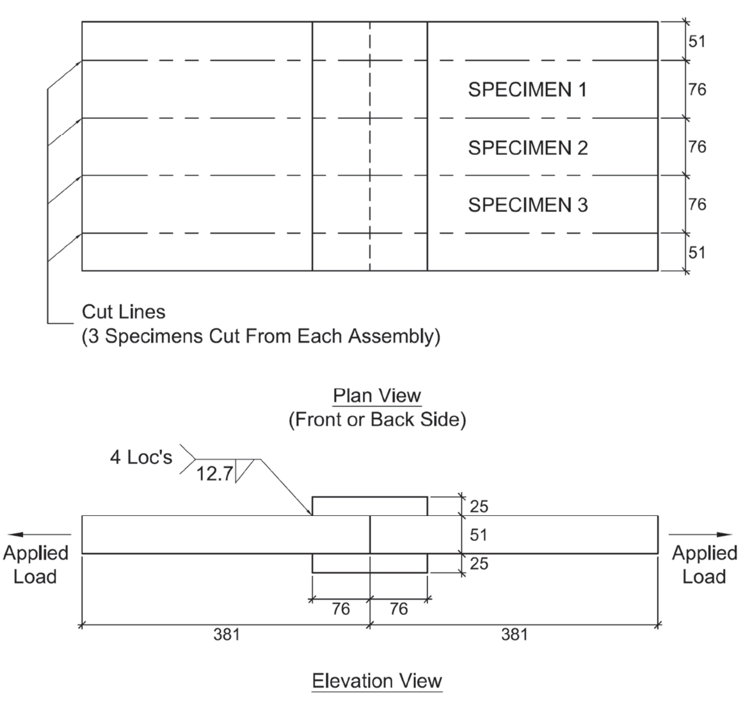

Fig. 5. Complementary test transverse weld (T) specimen.

The fillet weld deformations measured in the complementary tests were used to establish fillet weld load–deformation response curves. Since the complementary tests are used to model the assumed behavior of the individual segments of the tested MOFW connections, these response curves are used to predict the capacities of the MOFW connections.

After each test was complete, the fracture surface of the test fillet welds from each specimen was measured. In this way the degree of root penetration, the fracture angle, and the fracture throat area were assessed.

EXPERIMENTAL RESULTS

As previously stated, although all the test specimens were fabricated with E70T-7 wire, specimens TL50, TL50a, TF and TFa were fabricated with one heat (Heat 1) and the remainder were fabricated with another (Heat 2). The results of three all-weld-metal tensile tests for each of the two heats showed that the Heat 1 wire had an average tensile strength (UTS) of 575 MPa and the Heat 2 wire had an average tensile strength of 569 MPa.

The results of the tests carried out on the longitudinal fillet weld ("L100" and "L150" specimens) and transverse fillet weld specimens ("T" specimens) are given in Table 6. Test results reported by Deng et al. (2006) are also provided in Table 6 since these data are also used to analyze the MOFW connection test results.

The test capacities given in Table 6 have been normalized at two levels in order to facilitate direct comparisons and to allow for the analysis of the MOFW test specimens. The first normalization is to account for the fillet weld throat area, represented by P/A_{throat} in Table 6. The values of P/A_{throat} are calculated by dividing the ultimate capacity of the specimen by the minimum throat area of the test welds. The minimum throat area is the length of the fillet weld segment multiplied by the segment's minimum throat dimension (MTD) determined from the measured leg sizes. The second normalization takes into account the tensile strength of the weld metal used to fabricate the specimen and is termed the normalized P/A_{throat} in Table 6. The normalized P/A_{throat} value is calculated by dividing the P/A_{throat} value by the weld metal's tensile strength.

The normalized values of the fillet weld deformation are given in the last column of Table 6, represented by Δ/d^*, where Δ is the weld deformation measured in the direction of the applied load and d^* is defined as follows:

Table 2. TL Specimen Weld Sizes and Calculated Throat Size										
Specimen	Segment	Front				Back				
		Fillet Weld Leg Size		Segment Length (mm)	MTD* (mm)	Fillet Weld Leg Size		Segment Length (mm)	MTD* (mm)
		MPL* (mm)	LPL* (mm)			MPL* (mm)	LPL* (mm)		
TL50-1	1	15.7	11.5	51.4	9.3	14.1	10.0	51.3	8.2
	2	16.4	12.3	76.2	9.8	16.0	11.0	76.1	9.0
	3	12.9	12.9	51.2	9.1	12.8	11.6	51.2	8.6
TL50-2	1	13.7	12.2	51.4	9.1	13.5	10.3	50.2	8.2
	2	15.2	11.9	76.4	9.4	13.5	11.9	77.0	8.9
	3	14.9	12.2	51.2	9.4	13.1	11.9	52.5	8.8
TL50-3	1	14.2	10.7	52.1	8.5	14.0	11.1	50.6	8.7
	2	15.3	12.8	76.3	9.8	15.3	11.8	76.7	9.3
	3	11.9	12.9	51.7	8.8	12.8	9.8	50.8	7.8
TL50-4	1	17.1	10.2	53.0	8.8	13.1	11.3	52.4	8.5
	2	18.3	11.0	78.4	9.4	15.8	11.2	76.6	9.1
	3	13.7	11.8	51.5	8.9	14.6	11.8	51.6	9.1
TL50a-1	1	9.6	7.8	51.0	6.1	8.4	7.4	50.9	5.5
	2	10.7	8.3	75.8	6.6	10.7	8.2	76.2	6.5
	3	9.2	8.4	51.2	6.2	8.6	8.5	52.1	6.0
TL50a-2	1	9.6	7.8	51.2	6.0	9.2	8.5	50.8	6.3
	2	10.6	8.3	76.2	6.6	11.3	8.2	76.8	6.6
	3	9.8	8.2	51.0	6.3	10.0	8.4	51.4	6.4
TL50a-3	1	8.4	7.5	50.1	5.6	9.0	9.2	50.2	6.4
	2	10.7	8.2	76.5	6.5	10.1	9.0	75.6	6.7
	3	9.7	8.0	51.8	6.2	9.7	8.3	50.3	6.3
TL50a-4	1	10.0	8.5	52.7	6.4	10.8	8.7	50.3	6.8
	2	11.8	9.1	78.3	7.2	12.3	7.9	78.2	6.7
	3	9.1	9.6	51.7	6.6	10.0	9.4	51.4	6.9
TL100-1	1	13.9	12.9	97.9	9.5	14.5	12.9	96.9	9.7
	2	17.1	12.4	76.6	10.0	17.5	13.0	77.0	10.4
	3	15.1	13.9	98.1	10.2	16.4	13.9	100.9	10.6
TL100-2	1	14.1	10.6	98.8	8.5	15.4	12.6	98.7	9.7
	2	14.6	11.0	78.0	8.8	16.7	11.9	75.6	9.7
	3	13.5	10.6	99.4	8.4	15.3	11.5	100.8	9.2
TL100-3	1	13.8	12.5	98.9	9.3	12.5	11.5	102.0	8.5
	2	16.8	12.6	77.2	10.1	15.7	10.8	76.0	8.9
	3	13.7	13.0	99.3	9.4	14.0	10.3	101.9	8.3

* Refer to Figure 6 for the definition of these acronyms.

Table 3. TF Specimen Weld Sizes and Calculated Throat Size									
Specimen	Segment	Front				Back			
		Fillet Weld Leg Size		Segment Length (mm)	MTD* (mm)	Fillet Weld Leg Size		Segment Length (mm)	MTD* (mm)
		MPL* (mm)	LPL* (mm)			MPL* (mm)	LPL* (mm)		
TF-1	1	12.9	10.5	66.1	8.1	14.4	11.6	64.6	9.0
	2	14.2	11.6	62.8	9.0	13.7	12.3	60.9	9.1
	3	14.4	11.0	62.9	8.7	14.8	13.2	69.6	9.9
TF-2	1	12.4	13.6	66.2	9.2	12.5	12.6	60.8	8.9
	2	15.0	13.6	61.2	10.1	13.6	12.7	66.0	9.3
	3	13.2	13.7	63.2	9.5	13.5	12.5	62.7	9.2
TF-3	1	13.9	12.1	64.7	9.1	12.2	12.0	68.0	8.5
	2	13.5	11.8	65.0	8.9	13.1	11.6	62.1	8.7
	3	13.2	11.2	61.5	8.5	12.4	11.3	60.7	8.3
TF-4	1	14.3	11.7	63.6	9.0	14.8	12.5	62.0	9.5
	2	17.1	11.6	65.9	9.6	16.8	12.6	65.7	10.1
	3	13.7	10.8	58.2	8.5	15.4	12.5	60.9	9.7
TFa-1	1	9.4	8.7	56.8	6.4	8.4	7.5	66.8	5.6
	2	9.2	9.2	64.9	6.5	9.6	8.2	60.8	6.2
	3	9.0	8.8	68.2	6.3	9.1	8.4	64.2	6.2
TFa-2	1	9.4	8.2	61.4	6.2	8.4	7.5	60.6	5.6
	2	9.5	8.0	62.5	6.1	8.9	7.7	61.1	5.8
	3	9.6	8.8	64.0	6.5	9.0	7.1	67.1	5.6
TFa-3	1	9.0	8.3	57.9	6.1	8.9	8.1	65.5	6.0
	2	9.0	8.5	65.8	6.2	9.2	7.7	61.0	5.9
	3	8.8	8.1	67.4	6.0	9.1	8.2	65.9	6.1
TFa-4	1	9.3	9.6	62.4	6.7	8.5	9.4	61.5	6.3
	2	9.6	9.9	64.8	6.9	8.8	9.2	65.5	6.3
	3	8.5	9.3	61.3	6.3	8.4	7.4	60.0	5.5

* Refer to Figure 6 for the definition of these acronyms.

$$d^* = d\left(\sin(\theta) + \cos(\theta)\right) \qquad (1)$$

where θ is the angle of the fillet weld axis from the load direction, and d is the measured MPL fillet weld leg size. For transverse and 45° fillet welds the dimension d^* represents the weld leg size measured in the direction parallel to the applied load, and for longitudinal welds it represents the leg size, as shear deformation dominates. This dimension is introduced for reasons explained later.

The test results for the TL and TF specimens are shown in Table 7. The minimum throat areas are given for each specimen's transverse and nontransverse (i.e., longitudinal segments in the TL specimens and 45° segments in the TF specimens) weld segments. It should be noted that the throat areas given in Tables 6 and 7 are adjusted to account for which weld segments failed. For example, if all the welds on the front lap plate of the specimen failed, but none failed on the back lap plate, then the throat area reported is twice the front fillet weld throat area.

Table 4. Longitudinal Fillet Weld Specimen Weld Sizes and Calculated Throat Size					
Specimen	Segment No.	Fillet Weld Leg Size		Segment Length (mm)	MTD* (mm)
		MPL* (mm)	LPL* (mm)		
L100-1	1	12.9	12.2	98.2	8.9
	2	12.3	11.3	98.9	8.3
	3	12.3	11.6	100.8	8.4
	4	12.9	12.0	99.6	8.8
L100-2	1	14.7	12.6	99.3	9.6
	2	14.2	10.9	98.2	8.7
	3	13.1	11.7	99.6	8.7
	4	13.8	10.6	100.0	8.4
L100-3	1	13.4	12.8	101.6	9.2
	2	13.7	12.7	103.2	9.3
	3	12.3	13.0	102.0	8.9
	4	13.1	12.9	101.2	9.2
L150-1	1	12.6	11.2	150.0	8.4
	2	12.4	12.3	148.7	8.7
	3	14.0	11.6	150.6	8.9
	4	13.4	12.3	149.7	9.1
L150-2	1	13.5	11.4	150.8	8.7
	2	13.0	11.8	148.3	8.7
	3	13.0	11.3	151.6	8.5
	4	13.2	11.0	152.1	8.5
L150-3	1	12.6	10.5	151.7	8.1
	2	12.3	10.4	150.7	7.9
	3	12.9	10.8	147.3	8.3
	4	12.8	11.2	148.2	8.4

* Refer to Figure 6 for the definition of these acronyms.

Table 5. Transverse Fillet Weld Specimen Weld Sizes and Calculated Throat Size					
Specimen	Front/Back	Fillet Weld Leg Size		Segment Length (mm)	MTD* (mm)
		MPL* (mm)	LPL* (mm)		
T-1	Front	13.4	12.2	76.3	9.0
	Back	13.9	12.3	76.3	9.2
T-2	Front	13.9	12.0	76.2	9.1
	Back	14.0	12.1	76.3	9.1
T-3	Front	14.5	12.0	76.3	9.3
	Back	13.6	12.5	76.3	9.2

* Refer to Figure 6 for the definition of these acronyms.

Table 6. SOFW Connection Test Results from Current Research and Deng et al. (2006)							
Specimen	Fillet Weld Angle, θ (Degrees)	Ultimate Capacity (kN)	A_{throat} (mm²)	Weld Metal UTS (MPa)	P/A_{throat} (MPa)	Normalized P/A_{throat}	Ultimate Δ/d*
T-1	90°	1005	1373	569	732	1.29	0.0309
T-2		1026	1386	569	740	1.30	0.0285
T-3		1088	1406	569	774	1.36	0.0312
F1-1	45°	789	1169	631	675	1.07	0.0928
F1-2		763	973	631	783	1.24	0.0818
F1-3		745	987	631	755	1.20	0.1103
F2-1		813	995	605	816	1.35	0.1245
F2-2		840	1068	605	787	1.30	0.1003
F2-3		823	1003	605	820	1.36	0.1412
F3-1		755	1092	493	691	1.40	0.1427
F3-2		725	1062	493	683	1.38	0.1193
L1-1	0°	731	1447	631	505	0.80	0.1775
L1-2		762	1582	631	482	0.76	0.1529
L1-3		740	1476	631	502	0.80	0.1503
L2-1		830	1548	605	536	0.89	0.1491
L2-2		805	1461	605	551	0.91	0.1267
L2-3		802	1464	605	548	0.91	0.1544
L3-1		743	1451	493	512	1.04	0.2083
L3-2		700	1467	493	477	0.97	0.1477
L3-3		750	1467	493	511	1.04	0.1982
L100-1		1470	3383	569	434	0.76	0.0910
L100-2		1469	3422	569	429	0.75	0.0983
L100-3		1780	3746	569	475	0.83	0.1229
L150-1		2263	4997	569	453	0.80	0.1264
L150-2		2431	4864	569	500	0.88	0.1380
L150-3		2473	4766	569	519	0.91	0.1522

ANALYSIS AND DISCUSSION

Two methods of analyzing a MOFW connection are discussed herein. The first method, referred to as the strength summation approach, assumes that the capacity of a MOFW connection is the sum of the capacities of each of the individual weld segments that make up the connection. The primary assumption of this method is that all of the weld segments have sufficient deformation capacity to allow each segment to reach its individual capacity. The second method, referred to as the compatibility approach, examines how the differences in ductility of the various segments in a MOFW connection limit the contribution of the noncritical weld segment to the connection capacity. The critical segment in a MOFW connection is the segment that has an orientation closest to 90° to the applied load, and the noncritical segments are the remaining segments.

Using the measured properties of SOFW connection specimens from the current research and that of Deng et al. (2006), the strength summation approach is used to predict the TL and TF specimen capacities. Only properties from SOFW connection specimens that used the same electrode classification (E70T-7) as the TF and TL specimens were used, which includes all the specimens in Table 6 except the F1, F3, L1 and L3 series. Thus, the mean normalized P/A_{throat} values used for the analysis are 0.85, 1.34 and 1.31 for longitudinal, 45° and transverse weld segments, respectively. It should be noted that all of the specimens in Table 6 were fabricated with nominal 12.7 mm (½ in.) fillet welds made with three passes. However, as discussed by Ng et al. (2004)

Table 7. MOFW Connection Test Results						
Specimen	Ultimate Load (kN)	Throat Area, A_{throat} (mm^2)		Weld Metal UTS (MPa)	Test-to-Predicted Ratios	
		Transverse Weld Segment	Nontransverse Weld Segment		Prediction 1	Prediction 2
TF-1	2003	1121	2538	575	0.72	0.87
TF-2	2508	1229	2325	575	0.92	1.10
TF-3	2228	1118	2202	575	0.88	1.05
TF-4	2429	1325	2365	575	0.86	1.03
TFa-1	1544	801	1561	575	0.69	0.83
TFa-2	1734	738	1509	575	0.81	0.98
TFa-3	1840	769	1548	575	0.84	1.01
TFa-4	1704	861	1520	575	0.76	0.90
TL50-1	1484	1436	1804	575	0.76	0.83
TL50-2	1664	1406	1824	575	0.85	0.94
TL50-3	1573	1465	1735	575	0.81	0.88
TL50-4	1700	1437	1846	575	0.86	0.94
TL50a-1	1299	993	1222	575	0.78	0.85
TL50a-2	1186	1009	1280	575	0.69	0.76
TL50a-3	1213	1004	1239	575	0.72	0.79
TL50a-4	1472	1084	1373	575	0.80	0.87
TL100-1	2359	1602	4009	569	0.75	0.86
TL100-2	2218	1461	3779	569	0.76	0.87
TL100-3	1976	1552	3706	569	0.67	0.76

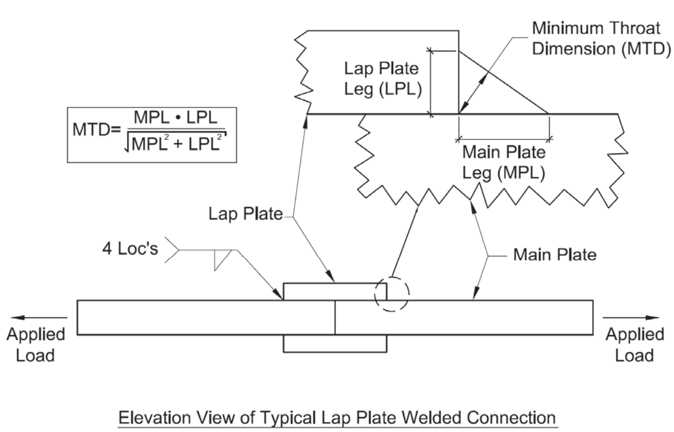

Fig. 6. Fillet weld leg size measurement definitions.

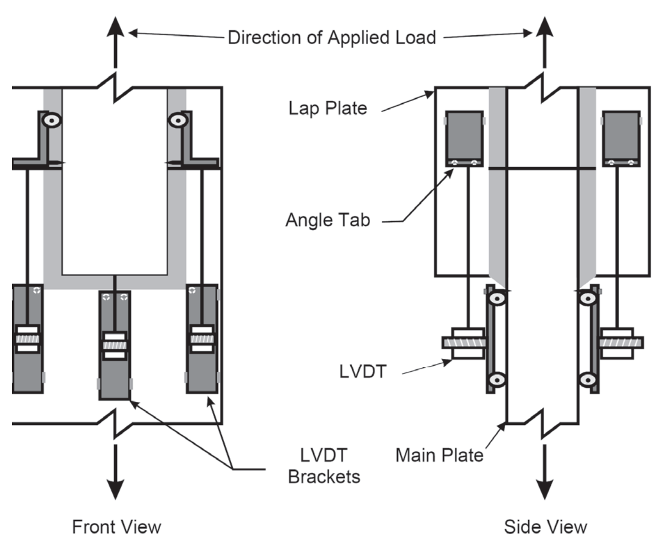

Fig. 7. Typical test specimen instrumentation and setup.

Table 8. Weld Size Effect for E70T-7 Electrodes (based on Ng et al., 2004)						
Specimen	Nominal Leg Size (mm)	P_m/A_{throat} (MPa)	Weld Metal UTS (MPa)	Normalized P_m/A_{throat}		Weld Size Effect
				Individual Assemblies	Mean	
T11	6.35	930	605	1.54	1.56	1.24
T12	6.35	1021	631	1.62		
T13	6.35	964	584	1.65		
T14	6.35	930	652	1.43		
T15	6.35	1015	652	1.56		
T25	12.7	783	605	1.30	1.26	
T26	12.7	822	631	1.30		
T27	12.7	710	584	1.22		
T28	12.7	788	652	1.21		

the unit strength of fillet welds is not independent of leg size. This can be seen in Table 8, where the average fillet weld unit strength of the specimens fabricated with 6.35-mm (¼-in.) welds is shown to be 1.24 times greater than the fillet weld unit strength of the specimens fabricated with 12.7-mm (½-in.) welds (three passes). To account for the greater unit strength expected of single-pass welds, the P/A_{throat} values in Table 6 are multiplied by the same ratio presented in Table 8, namely, 1.24, when predicting the TLa and TFa specimen capacities. However, it should be noted that the value of 1.24 is accounting for the variation in fillet weld unit strength as result of weld size and number of passes. Therefore, the 1.24 value is an upper bound for the TLa and TFa capacity predictions as the nominal fillet weld size in these specimens is 7.9 mm (5⁄16 in.), whereas the value was obtained from a comparison between 12.7-mm (½-in.) and 6.35-mm (¼-in.) nominal fillet weld sizes: thus, the true value may be somewhat lower.

Using the measured throat areas of the TL and TF specimens given in Table 7 and the P/A_{throat} values as described in the preceding paragraph, the capacity of each weld segment is calculated. The strength summation approach then predicts the TL or TF connection capacity by summing each weld segment's individual capacity. Using the strength summation approach, the test-to-predicted ratio for each of the TL and TF specimens is shown in Table 7 under Prediction 1. Figure 8 compares the test and predicted capacities using the strength summation approach and presents the associated mean test-to-predicted ratio and coefficient of variation. It is clear that the strength summation method provides a nonconservative prediction of MOFW connections.

The second method used to predict the capacity of a MOFW connection is the compatibility approach. Several research programs have verified that the deformation capacity of a fillet weld changes with a variation in loading angle: generally the closer the fillet weld orientation gets to 90° from the load direction, the smaller is its deformation capacity. The compatibility approach shows how this variation in fillet weld deformation capacity affects the capacity of MOFW connections. Figure 9 shows the fillet weld deformation of SOFW connections from this research, as well as that of Deng et al. (2006) and Miazga and Kennedy (1989). The figure reports the data in terms of Δ_{ult}/d^*, where Δ_{ult} is the deformation of the fillet weld at its ultimate capacity and d^* is as defined in Equation 1. The weld deformations reported by Miazga and Kennedy (1989) were normalized by dividing by the fillet weld leg size, d. The weld deformations given by Deng et al. (2006) were normalized by dividing by the leg size, d, only for orientations 0° and 90° and the deformations for welds with an orientation of 45° were normalized by dividing by $d\sqrt{2}$ (the weld dimension in the direction of loading). Since $d^* = d\sqrt{2}$ when $\theta = 45°$, using d^* allows a direct

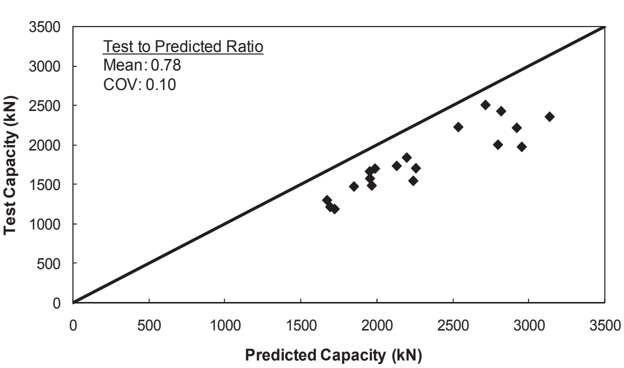

Fig. 8. Strength summation approach predictions.

comparison between the test data given by Miazga and Kennedy (1989) and that given by Deng et al. (2006). It should be noted that all the test data shown in Figure 9 were obtained using specimens whose plates remained elastic during the test, as the weld deformations with yielding base metal reported by Ng et al. (2004) were significantly larger.

There is significant scatter shown in the Δ_{ult}/d^* values in Figure 9 at weld orientations of 0° and 45°. The inconsistency in the two research programs at 45° suggests the need to look at two different predictions on the variation in weld deformation capacity with respect to the load angle, θ. A power relationship, similar to that presented in Lesik and Kennedy (1990), provides a good fit to the data when the 45° weld deformations from Deng et al. (2006) are not considered:

$$\frac{\Delta_{ult}}{d^*} = 0.20(\theta + 2)^{-0.36} \tag{2}$$

However, a linear relationship may be more appropriate when considering only the results of the current research and that of Deng et al. (2006):

$$\frac{\Delta_{ult}}{d^*} = 0.146 - 0.0013\theta \tag{3}$$

Other research projects, such as those of Butler et al. (1972) and Lesik and Kennedy (1990), have reported a nonlinear relationship between the load angle and fillet weld deformation capacity; however, the large scatter in test results at θ = 45° warrants considering both Equations 2 and 3.

A family of load–deformation response curves is a necessary component of the compatibility approach. Using the test results from the complementary test program and the test data from the tests of Deng et al. (2006), a general fillet weld response curve similar to the one given in Lesik and Kennedy (1990) was developed by Callele et al. (2005). The two curves—that of Callele et al. (2005) and that of Lesik and Kennedy (1990)—are shown in Figure 10. The difference between the two response curves is likely a result of the differences in fabrication technique of the test specimens from the two experimental programs. The load–deformation response curves developed by Callele et al. (2005) take the following mathematical form:

when ρ > 0.05,

$$\frac{P_\theta}{P_{U\theta}} = 1.47\rho - 95.42\,\rho^{1/2} + 887.57\rho^{1/3} - 2724.66\,\rho^{1/4} + 3286.37\rho^{1/5} - 1354.33\,\rho^{1/6} \tag{4}$$

when ρ ≤ 0.05,

$$\frac{P_\theta}{P_{U\theta}} = 8.476\rho \tag{5}$$

where

$$\rho = \frac{\Delta}{\Delta_{ult}} \tag{6}$$

The value $P_\theta/P_{U\theta}$, which is valid for an arbitrary θ, is the fraction of a weld segment's ultimate capacity mobilized by a particular normalized deformation, ρ.

Due to the complexity of Equation 4, a simpler form of the response curve has been developed as follows:

when ρ > 0.07,

$$\frac{P_\theta}{P_{U\theta}} = \left[\rho(2-\rho)\right]^{.25} \tag{7}$$

when ρ ≤ 0.07,

$$\frac{P_\theta}{P_{U\theta}} = 8.7\rho \tag{8}$$

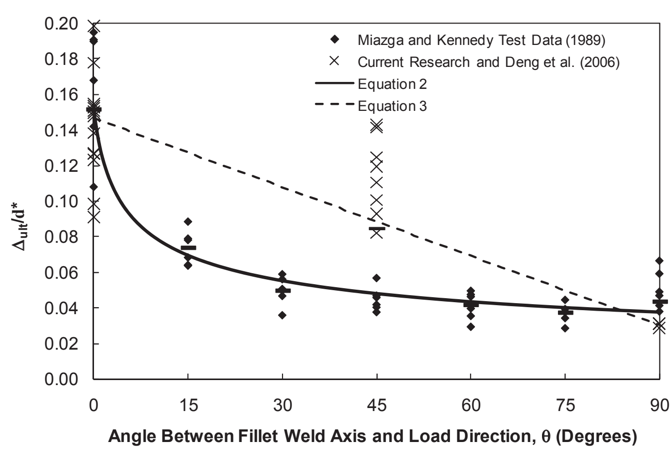

Fig. 9. Fillet weld ductility test data.

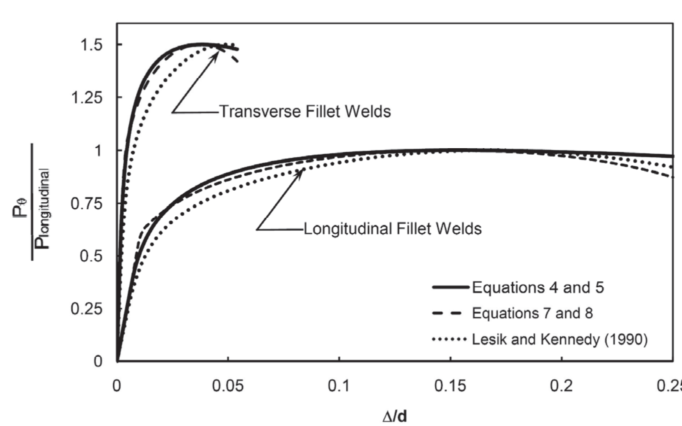

Fig. 10. Fillet weld load–response curves.

The form of Equation 7 is identical to that currently used by AISC—Equation J2.8 of the AISC *Specification* (AISC, 2005)—however, the coefficients in the equation have been modified to fit Equation 4. Though unnecessary for this analysis, Equation 8 has been provided to give an accurate description of the load–deformation response over the entire deformation range. Equations 7 and 8 are much simpler to use than Equations 4 and 5, yet as seen in Figure 10 the two sets of curves have good agreement, particularly up to the peak capacity. Thus, Equations 7 and 8 will be used in this analysis.

With estimates of both fillet weld deformation capacity and load–deformation response, the compatibility approach is now employed to estimate the TF and TL specimens' capacities. The maximum force that each weld segment could contribute to the connection capacity is calculated in the same manner as in the strength summation approach, except that in the compatibility approach the noncritical weld segment capacities are reduced by the calculated value of $P_\theta/P_{U\theta}$.

The value of $P_\theta/P_{U\theta}$ is determined by assuming that the capacity of a MOFW connection is reached when the Δ_{ult} deformation of the critical weld segment is reached. By assuming rigid body movement of the connection plates, the corresponding fillet weld deformation of a noncritical segment, (Δ/d^*), can be shown (Callele et al., 2005) to be a function of the weld deformation in the critical weld segment, (Δ_{ult}/d^*), and the filletweld orientations θ_1 and θ_2 of the noncritical and critical segments, respectively. Thus the deformation in the noncritical weld segment at the point where the critical weld segment reaches its deformation limit of (Δ/d^*) is:

$$\left(\frac{\Delta}{d^*}\right)_1 = \left(\frac{\Delta_{ult}}{d^*}\right)_2 \left(\frac{\sin(\theta_2)+\cos(\theta_2)}{\sin(\theta_1)+\cos(\theta_1)}\right) \tag{9}$$

Combining Equation 9 with a prediction of the weld segment's deformation, either by measured test results or Equations 2 or 3, the value of ρ for the noncritical segment is calculated. This value of ρ is then used with Equations 7 and 8 to calculate the fraction of the noncritical weld segment's maximum force that will contribute to the connection capacity. This fraction of the maximum force is referred to herein as the noncritical weld segment's strength reduction factor, M_w. The products of each noncritical segment's strength reduction factor and ultimate capacity are summed, along with the ultimate capacity of each critical weld segment, to predict the total MOFW connection capacity.

The compatibility approach procedure is used to predict the capacities of the TL and TF specimens using the measured strength and deformation values from specimens fabricated from E70T-7 wires from the current research and the test data from Deng et al. (2006). The test-to-predicted ratios for the TL and TF specimens are shown in Table 7 under Prediction 2. The comparison between the test and predicted values is shown in Figure 11. The mean test-to-predicted ratio of 0.90 represents a significant improvement over the strength summation approach. However, given that capacities of the TLa and TFa specimens were predicted using an upper-bound value to account for higher weld unit strengths in the 7.9-mm (5⁄16-in.) single-pass welds, the compatibility approach may give a better prediction of the MOFW connection capacities than the test-to-predicted ratio of 0.90 indicates.

The calculated values of M_w using measured values for weld strength and deformation capacity are 0.80 and 0.75 for the longitudinal fillet weld segments and 45° weld segments, respectively, when combined with a transverse weld. The smaller value of M_w for the 45° weld segments is the result of larger than expected measured Δ_{ult}/d^* values for the F2 specimens of Deng et al. (2006). The larger Δ_{ult}/d^* decreased the value of ρ, which therefore decreased the value of M_w for the 45° weld segments.

In spite of the fact that the compatibility approach does improve upon the prediction of the TL and TF specimen capacities as compared to the summation approach, it is still seen to overestimate the capacities. Therefore, to assess whether or not the compatibility approach is appropriate for design, it is necessary to perform a reliability analysis on the test data with an equation that takes into account the compatibility approach.

In order to use the compatibility approach in design, it is desirable to assess the variation in M_w for different noncritical weld segment orientations. This assessment is done for a transverse critical weld orientation in Figure 12 using the simplified response curve of Equations 7 and 8 along with the predicted weld deformations of both Equations 2 and 3. However, it would be too cumbersome to go through the compatibility approach for every weld connection design. Therefore, the following equation is proposed to simplify the evaluation of M_w, as it is a function only of the load angles

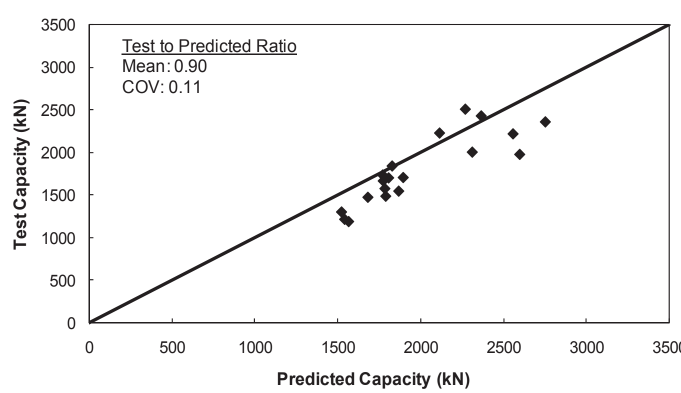

Fig. 11. Compatibility approach capacity predictions.

θ_1 and θ_2 of the weld under consideration (either critical or non-critical) and critical weld segments, respectively:

$$M_w = \frac{0.85 + \theta_1/600}{0.85 + \theta_2/600} \quad (10)$$

In addition to simplifying the design procedure greatly, Equation 10 tends to balance the significantly different curves for M_w obtained from Equations 2 and 3 shown in Figure 12. It is also consistent with the current Equation J2-9b in the AISC *Specification* (AISC, 2005) that is for the special case of combined transverse and longitudinal welds, but it eliminates the need for Equation J2-9a that acknowledges neither the higher strength of transverse welds nor the effect that the variation in deformation capacity with respect to weld orientation has on the strength of MOFW connections. Although the calculated value of M_w for a noncritical longitudinal weld segment is about 8% less than the value (0.85) from Equation 10, the equation is shown subsequently to provide an adequate margin of safety for design.

A reliability analysis was performed on the TL and TF test data to determine the reliability index obtained using the proposed design procedure and current resistance factors. The full details of this analysis can be found in Callele et al. (2005); however, a summary of the key parameters is provided in Table 9. For determining predicted values, both the Canadian design standard and the AISC *Specification* are considered, combined with the strength reduction factor, M_w, defined in Equation 10. The former design equation becomes:

$$V_r = 0.67\phi_w A_w X_u (1.00 + 0.50 \sin^{1.5}\theta) M_w \quad (11)$$

and the latter:

$$V_r = 0.67\phi A_w F_{EXX} (1.00 + 0.50 \sin^{1.5}\theta) M_w \quad (12)$$

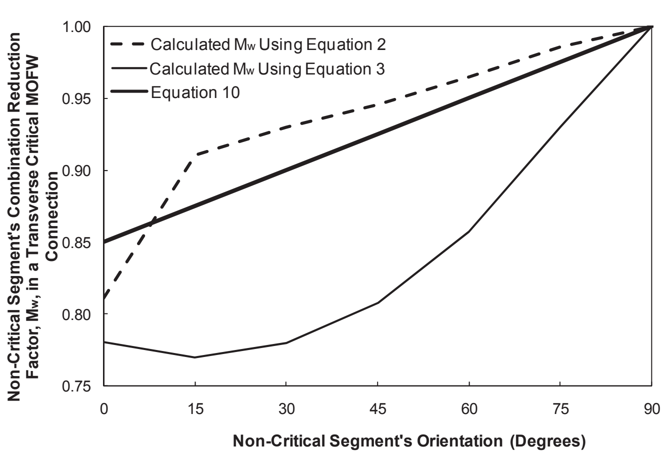

Fig. 12. Strength reduction factors for a MOFW connection with a transverse weld as the critical weld segment.

Table 9. Reliability Analysis Parameters

	Strength Summation Approach	Compatibility Approach
ρ_G	1.03	1.03
V_G	0.10	0.10
ρ_{M1}	1.15	1.15
V_{M1}	0.08	0.08
ρ_{M2}	1.23	1.23
V_{M2}	0.12	0.12
ρ_P	0.83	0.89
V_P	0.12	0.11
ρ_R	1.21	1.30
V_R	0.22	0.21
$\Phi(\beta)$	0.90	0.87
β	4.1	4.5

Because the product $0.67\phi_w = 0.60\phi$, where $\phi_w = 0.67$ and $\phi = 0.75$, predicted MOFW connection capacities—and, therefore, the resulting reliability index—are identical for the two equations. It should be noted that in the reliability analysis, only Equations 11 and 12 were used in the evaluation of the professional factor, ρ_P, and that the base metal strength at the fusion face, currently a required weld strength check in both design specifications, was not considered.

The reliability analysis of the strength summation approach simply uses $M_w = 1.0$ for all weld segments in a MOFW connection. Conversely, the compatibility approach predicts the capacity of a MOFW connection as the sum of each weld segment's capacity evaluated using Equation 11 or 12 with M_w as defined in Equation 10. The strength summation and compatibility methods result in reliability indices of 4.1 and 4.5, respectively. Considering that welded connections have small deformation capacities when compared with typical main structural elements, a reliability index of 4.0 to 4.5 is considered more suitable as a target (as compared with a reliability index of 3.0 for main members). Although both the strength summation and compatibility methods provide a reliability index within the target range, the use of Equation 10 is recommended for the following two reasons. The first is that the average test-to-predicted ratio of the strength summation method is very low, which indicates that this method does not accurately model MOFW connection behavior. The second reason to use Equation 10 is that the common MOFW connection of a welded joint that includes both transverse and longitudinal fillet welds is most susceptible to the differences in fillet weld deformation capacity. The longitudinal weld capacity has been shown to be reduced by about 20% (see Figure 12), which points to a significant deficiency of the strength summation method. The use of Equation 10 with the accepted North American design provisions for fillet weld strength is therefore recommended for use in the design of MOFW connections. Although tests where the critical weld is not transverse to the load direction were not considered in the reliability analysis, an extension to these cases in order to generalize the procedure is reasonable since the concept of deformation compatibility is consistently applied.

As previously mentioned, the experimental research and derivation of Equation 10 have assumed that the fillet weld segments that comprise the MOFW connection have the same nominal size. However, for the case of MOFW connections with unequal leg sizes, the authors caution against the use of Equation 10 when the less ductile weld segment is smaller than the more ductile weld segment. When the less ductile weld segment is smaller, it is likely that the more ductile weld segment's capacity would be reduced more than Equation 10 predicts. In this case, Equation 9 could be modified as follows, where d_2 and d_1 are, respectively, the leg sizes of the less ductile and more ductile weld segments:

$$\left(\frac{\Delta}{d^*}\right)_1 = \left(\frac{\Delta_{ult}}{d^*}\right)_2 \left(\frac{\sin(\theta_2) + \cos(\theta_2)}{\sin(\theta_1) + \cos(\theta_1)}\right) \left(\frac{d_2}{d_1}\right) \qquad (13)$$

The deformation compatibility procedure described herein could then be applied using Equation 13 instead of Equation 9 and a different M_w value calculated. Muir (2008) gives additional considerations for cases where unequal weld sizes are used in the same joint.

It should also be noted that three recent reliability analyses have been carried out (Lesik and Kennedy, 1990; Deng et al., 2006; Callele et al., 2005) that have validated the use of Equations 11 and 12 for the prediction of fillet weld strength for any fillet weld orientation. However, current design procedures limit the use of these equations by requiring that the strength of the base material at the fusion face of the weld also be checked using virgin material properties that are not representative of the post-weld condition. This requirement effectively prevents the utilization of the full strength of fillet welds that approach 90° to the loading direction. Many test specimens used in the aforementioned reliability analyses exhibited a fracture surface that followed the fusion area between the fillet weld and base metal, yet Equations 11 and 12 were still shown to provide an adequate reliability index. It is, therefore, suggested that the check of the base metal strength along the fusion area is not required, provided matching electrodes are used. Removing this requirement would allow the designer to take advantage of the full 50% strength increase of transverse fillet welds over longitudinal fillet welds that has been observed in several research programs.

CONCLUSIONS AND RECOMMENDATIONS

By comparing test-to-predicted ratios and calculated reliability indices, the compatibility approach to the prediction of MOFW connection capacity has been shown to be superior to the predictions based on the strength summation approach. Therefore, Equations 10 and either 11 or 12 are recommended for design of concentrically loaded MOFW connections fabricated with equal-legged weld segments. The equations have been verified by comparison with 19 tests on MOFW connections fabricated with FCAW fillet welds. The design equations allow the evaluation of the capacity of any MOFW connection that is concentrically loaded.

Three recent research programs have verified the use of Equation 11 or 12 for the calculation of fillet weld design strength without the necessity for the designer to check the base metal strength on the fusion area. Therefore, it is also recommended that when matching electrodes are used for the fabrication of fillet welded connections, the base metal strength check be omitted and only Equation 11 or 12 be used.

ACKNOWLEDGMENT

This research was funded by the American Institute of Steel Construction and the Natural Sciences and Engineering Research Council of Canada. Their support is gratefully acknowledged.

REFERENCES

AISC (2005), *Specification for Structural Steel Buildings*, ANSI/AISC 360-05, American Institute of Steel Construction, Chicago, IL.

AWS (2005), *Specification for Carbon Steel Electrodes for Flux Cored Arc Welding*, ANSI/AWS A5.20/A5.20M:2005, American Welding Society, Miami, FL.

Butler, L.J., Pal, S. and Kulak, G.L. (1972), "Eccentrically Loaded Welded Connections," *Journal of the Structural Division*, ASCE, Vol. 98, No. ST5, May, pp. 989–1005.

Callele, L.J., Grondin, G.Y. and Driver, R.G. (2005), "Strength and Behaviour of Multi-orientation Fillet Weld Connections," Structural Engineering Report 255, Dept. of Civil and Environmental Engineering, University of Alberta, Edmonton, Alberta, Canada.

CSA (2001), "Limit States Design of Steel Structures," CSA S16-01, Canadian Standards Association, Toronto, Canada.

Deng, K., Grondin, G.Y. and Driver, R.G. (2006), "Effect of Loading Angle on the Behavior of Fillet Welds," *Engineering Journal*, AISC, Vol. 43, No. 1, pp. 9–23.

Lesik, D.F. and Kennedy, D.J.L. (1990), "Ultimate Strength of Fillet Welded Connections Loaded in Plane," *Canadian Journal of Civil Engineering*, Vol. 17, No. 1, pp. 55–67.

Manuel, T.J. and Kulak, G.L. (2000), "Strength of Joints that Combine Bolts and Welds," *Journal of Structural Engineering*, ASCE, Vol. 126, No. 3, March, pp. 279-287.

Miazga, G.S. and Kennedy, D.J.L. (1989), "Behavior of Fillet Welds as a Function of the Angle of Loading," *Canadian Journal of Civil Engineering*, Vol. 16, No. 4, pp. 583–599.

Muir, L.S. (2008) "Deformational Compatibility in Weld Groups," Proceedings, *Connections in Steel Structures VI*, June 23-25, Chicago, IL.

Ng, A.K.F., Deng, K., Grondin, G.Y. and Driver, R.G. (2004), "Behavior of Transverse Fillet Welds: Experimental Program," *Engineering Journal*, AISC, Vol. 41, No. 2, pp. 39–54.